Available online at www.sciencedirect.com
SCIENCE DIRECT
Tetrahedron: Asymmetry
Tetrahedron: *Asymmetry* 17 (2006) 1387–1393

# Assignment of the absolute configuration of (+)-5,5′,6,6′-tetrahydro-7,7′-spiro[7*H*-cyclopenta[*b*]pyridine], a new inherently chiral spiropyridine, by a nonempirical analysis of its circular dichroism spectrum

Michele Claps,[a] Nunziatina Parrinello,[c] Carlos Saá,[b] Jesús A. Varela,[b] Salvatore Caccamese[c,*] and Carlo Rosini[a,*]

[a]*Dipartimento di Chimica, Università della Basilicata, via Sauro 85, 85100 Potenza, Italy*
[b]*Departamento de Quimica Organica, Universidad de Santiago de Compostela, Avda. de las Ciencias, 15782 Santiago de Compostela, Spain*
[c]*Dipartimento di Scienze Chimiche, Università di Catania, viale Doria 6, 95125 Catania, Italy*

Received 29 March 2006; accepted 28 April 2006

**Abstract**—The absolute configuration of (+)-spiropyridine **1**, obtained in its enantiopure form by chromatographic resolution of the racemate upon the CSP Chiralcel AD, has been assigned as (a*S*) by simulating the ECD spectrum in the range 320–235 nm both by coupled oscillator (DeVoe) and TD DFT/B3LYP/6-31G* calculations.


## 1. Introduction

Spiranes possessing chiral $C_2$ symmetry are occasionally used as effective chiral ligands in catalytic asymmetric reactions. Some years ago, certain spiropyridines were obtained as racemic mixtures in a one-step method based on a Co(I)-catalyzed double cyclization between bis-alkyne-nitriles and alkynes.[1] Formula reports the structure of (a*S*)-5,5′,6,6′-tetrahydro-7,7′-spiro[7*H*-cyclopenta[*b*]pyridine], (a*S*)-**1,** (it is noteworthy that this name follows the Chemical Abstract nomenclature and it is different from that used in the Supporting information of Ref. 1) that was resolved into its enantiomers, which were characterized by qualitative CD spectra.[1] This is a potentially useful chiral catalyst and properly functionalized derivatives of it can be seen as building blocks for the construction of chiral macromolecules.

In addition, spiranes possessing molecular dissymmetry are intellectually intriguing as very few compounds of this kind have been fully characterized[2] in optically active form and important stereochemical information has been lacking.

(aS)-1

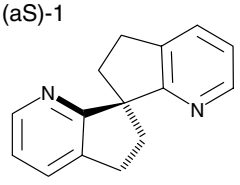


Due to the experience of some of us in the separation of the enantiomers of $C_2$-symmetric spirobiindanes[3] and calix[8]-arenes,[4] we tried the HPLC separation and isolation of the enantiomers of **1**. Furthermore, in the light of increasing interest in the analysis of chiroptical properties to determine the absolute configuration of flexible molecules, we attempted a nonempirical analysis of the CD spectrum of the isolated enantiomer **1** in order to establish the absolute configuration.

## 2. Results and discussion

### 2.1. Chiral separation and chiroptical properties

Table 1 shows the chromatographic results for the enantioseparation of spiropyridine **1** using as chiral stationary

* Corresponding authors. Tel.: +39 0971 202241 (C.R.); e-mail: rosini@unibas.it

0957-4166/$ - see front matter © 2006 Elsevier Ltd. All rights reserved.
doi:10.1016/j.tetasy.2006.04.034

phases two polysaccharide-derived CSP (Chiralcel OD and Chiralpak AD).

The use of Chiralpak AD affords a larger separation factor $\alpha$ than that obtained using Chiralcel OD, under the same experimental conditions as shown in lines 1 and 6 of Table 1 ($\alpha = 2.90$ and 1.20, respectively) or using a different alcohol in the mobile phase, as shown in lines 1 and 5. Using the conditions reported in line 1, a remarkable elution interval of almost 15 min between the two enantiomeric peaks was obtained. The separation factor was slightly affected by a variation in the flow rate of the mobile phase, as shown in lines 1–3 and in lines 4 and 5. Most significantly the resolution factor is quite high using the Chiralcel AD and this affords an overloading of the column to separate and to isolate the individual enantiomers. Typical enantiomeric separations, as a function of CSP and alcohol in the mobile phase are shown in Figure 1.

The difference in chiral recognition of cellulose and amylose derivatives is probably due to a different chiral environment around the carbamate residue and to the wider and more compact helix of the amylose derivative.[5] It is interesting to note that, in our experience, the Chiralpak AD CSP resulted much more effective in the enantiomeric resolution of other $C_2$-symmetric molecules, as spirobiindanes[3] and calix[8]arenes.[4]

Based on the chromatographic results in Table 1, we resorted to the experimental conditions in line 1 to perform the isolation of the enantiomers of spiropyridine **1**. This was accomplished by repeated 50 μL injections (0.1–0.2 mg) of racemic spiropyridine (20 mg) in EtOH. Collection of the eluates corresponding to the two chromatographic peaks gave, after filtration and evaporation, 9.2 mg of the first eluted peak and 7.1 mg of the second eluted one. The CD spectra of both compounds were measured and were shown to be mirror images of each other, indicating their enantiomeric nature.

Analytical HPLC reruns of the eluates indicated an enantiomeric excess (ee) of 99.5% for the first peak and 100% for the second one. A specific rotation of $[\alpha]_D^{22} = +4.2$ ($c$ 0.46, EtOH) was measured for the first eluted sample of **1**, while the second one afforded the experimental $[\alpha]_D^{22} = -6.5$ ($c$ 0.36, EtOH).

### 2.2. Stereochemical nomenclature

Nomenclature of the absolute configuration of the structure used in the theoretical calculation is based on the ste-

**Table 1.** Enantioselective HPLC resolution of the spiropyridine **1** on Chiralcel OD and Chiralpak AD

| CSP | A[a] (%) | FR[b] | $k_1'$[c] | $t_1$ | $t_2$ | $\alpha$ | $R_s$ |
|---|---|---|---|---|---|---|---|
| AD | 2-PrOH (5)[d] | 0.5 | 1.36 | 13.5 | 28.4 | 2.90 | 6.8 |
| AD | 2-PrOH (5) | 1.0 | 1.35 | 6.7 | 14.1 | 2.90 | 6.0 |
| AD | 2-PrOH (5) | 1.3 | 1.23 | 5.2 | 10.4 | 2.80 | 5.7 |
| OD | EtOH (20) | 0.7 | 0.47 | 5.4 | 5.7 | 1.16 | <0.5 |
| OD | EtOH (5) | 0.5 | 1.05 | 11.7 | 13.1 | 1.20 | 0.6 |
| OD | 2-PrOH (5) | 0.5 | 1.02 | 11.7 | 12.9 | 1.20 | 0.6 |

[a] Percentage of alcohol in *n*-hexane; UV detector at 280 nm.
[b] Flow rate (mL/min); $t_0$, min = 5.72 (AD at 0.5 mL/min), 2.85 (AD at 1 mL/min), 2.33 (AD at 1.3 mL/min), 5.73 (OD at 0.5 mL/min), 3.82 (OD at 0.7 mL/min).
[c] Capacity factor of the first eluted enantiomer.
[d] Experimental conditions used for semipreparative isolation.

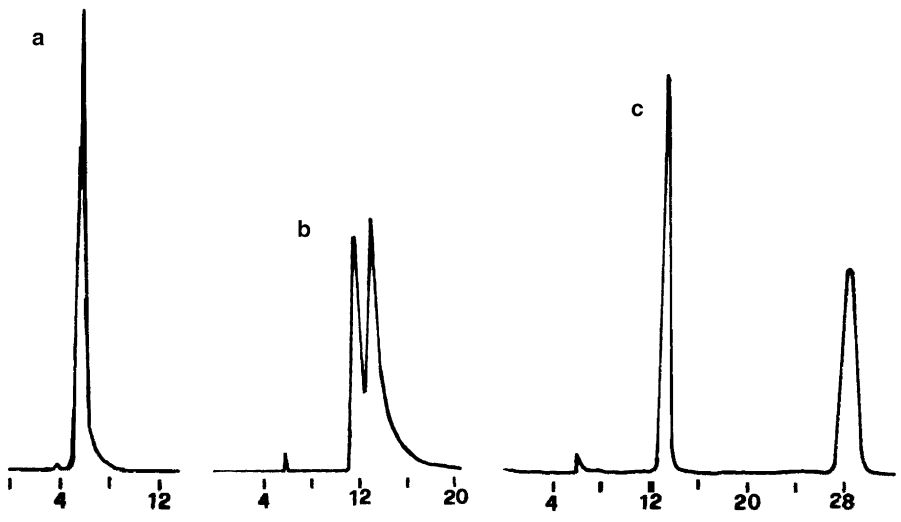


**Figure 1.** HPLC enantioseparation of spiropyridine **1**. Conditions: (a) column: Chiralcel OD, mobile phase: *n*-hexane/ethanol 80:20 at 0.7 mL/min; (b) Chiralcel OD, mobile phase: *n*-hexane/2-PrOH 95:5 at 0.5 mL/min; (c) Chiralpak AD, mobile phase: *n*-hexane/2-PrOH 95:5 at 0.5 mL/min.

reochemical descriptor (a*S*) to define axial chirality. Figure 2 shows the priority designation aiding to (a*S*)-configuration assignment. The priority sequence is 1 > 2 > 3 > 4 according to the rule of axial chirality (elongated tetrahedron).[6]

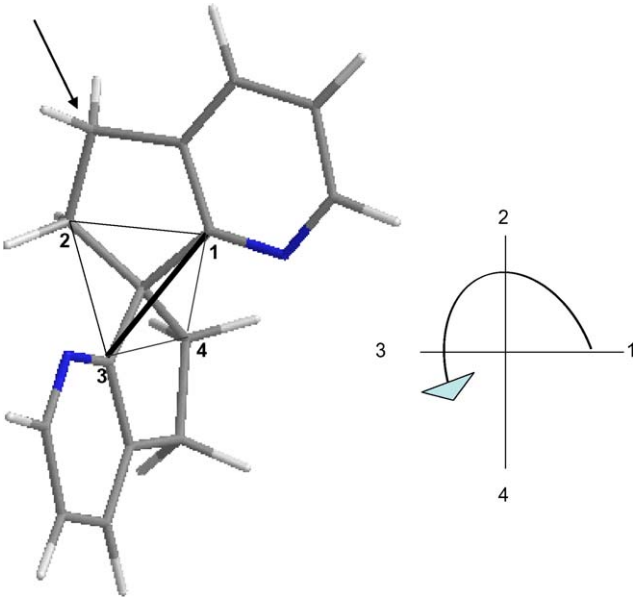


**Figure 2.** The (a*S*)-enantiomer according to the rule of axial chirality (elongated tetrahedron). Priority sequence 1 > 2 > 3 > 4.

Following this sequence and placing the lowest priority group 4 in the back, away from the observer, the sequence 1–2–3 gives a counterclockwise rotation and hence an (a*S*)-configuration for the structure used in the calculation. The stereochemical nomenclature of some type of spiranes can pose some problems, as has been carefully discussed in leading references.[7,8] The structure shown in Figure 2 has an (*R*)-configuration instead, according to the central chirality rule.[9] Thus, this is a typical example of different stereochemical assignment when the configuration is based on the rules of axial chirality rather than central chirality. A similar example where a depicted structure represents either an (a*S*)- or (*R*)-configuration is a 2,7-diazaspiro[4,4]nonane.[10] Nevertheless, this ambiguity is ruled out using the unequivocal helicity rule.[11] Indeed, the configuration shown in Figure 2 is the P enantiomer, because the correspondence of (a*S*) with P is a general rule.

### 2.3. Absorption and CD spectra of (+)-1

In order to arrive at a configurational determination, the absorption and circular dichroism (CD) spectra must be carefully analyzed and interpreted. The absorption and CD spectra of the first eluted enantiomer of (+)-**1**, are collected in Figure 3.

The UV absorption spectrum shows a broad band (between 300 and 240 nm), centred at about 270 nm ($\varepsilon_{max}$ 11,000 ca.), having a clear shoulder at 280 nm, $\varepsilon_{max}$ 9000 ca., and a less evident one at 265 nm. Below 240 nm, the absorption increases monotonically. In the CD spectrum, an intense Cotton effect with two maxima (at 275 and

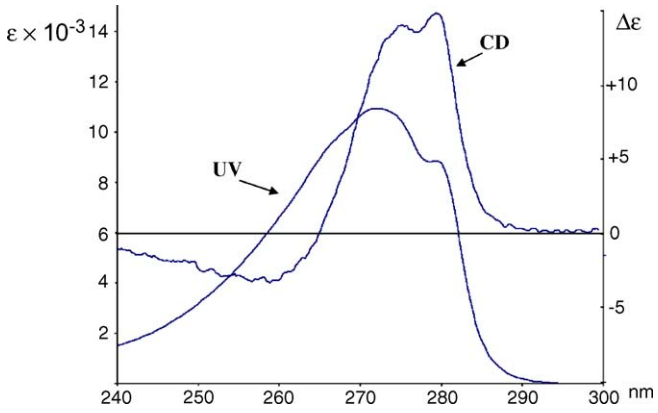


**Figure 3.** Absorption (UV) and CD spectra of (+)-**1** in ethanol.

280 nm) of the same intensity (Δε +13 ca.) can be observed. Such a Cotton effect is followed by a less intense CD band (Δε −3) at 260 nm. It is generally accepted[12–14] that the lowest energy region of the UV/CD spectra of the pyridine chromophore is dominated by the presence of two main electronic transitions, which are almost degenerate: a former one, which is n → π* in nature and a latter one, which is π → π* in nature. In the $C_{2v}$ point group of the pyridine chromophore and within the reference system reported in Chart 1 they become $^1A_1 \rightarrow {}^1B_1$ and $^1A_1 \rightarrow {}^1B_2$. In the $C_{2v}$ point group, they are both electrically and magnetically allowed, but, in this achiral point group, these transition moments are orthogonal so no optical activity occurs. In the reference system we have chosen:

$$^1A_1 \rightarrow {}^1B_1 \quad \mu_x; \quad m_y$$
$$^1A_1 \rightarrow {}^1B_2 \quad m_x; \quad \mu_y$$

this means that the first transition possesses an electric transition moment perpendicular to the pyridine plane and a magnetic transition moment in the aromatic plane, along *y*. The opposite is true for the π → π* transition. Taking into account that (+)-**1** can be considered, from a spectroscopic point of view, as a pyridine dimer and considering also that this chromophore possesses electrically allowed transitions, it obvious to think that an analysis of the CD spectrum of (+)-**1** within the exciton model[15–18] could afford the correct configurational assignment. Clearly in this case, we cannot use the simple 'exciton chirality rules' due to Harada and Nakanishi,[19–22] because in the case of (+)-**1**, we have two dipoles for each chromophore meaning that we have to treat the simultaneous interactions of four dipoles, whilst the above rules can be applied only in the case of two interacting dipoles. As a consequence, we have to use a more general exciton treatment;

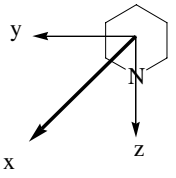


**Chart 1.**

from this point of view the DeVoe model[23–25] can be considered the most useful one.

### 2.4. DeVoe CD calculations

Here we report the most important features of the DeVoe model in order to understand how a practical calculation works and what are the necessary parameters. In the DeVoe model, a molecule is considered to be composed of a set of subsystems, the chromophores; these are polarized by the external electromagnetic radiation and are coupled to each other by their own dipolar oscillating fields. The optical properties (absorption, refraction, optical rotatory dispersion and circular dichroism) of the molecule under study can be calculated by taking into account the interaction of the subsystems. Therefore, this treatment requires a division of the molecule into a set of subsystems that have to be suitably characterized. Each group is then represented in terms of one (or more) classical oscillator(s); each oscillator represents an electric-dipole-allowed transition, defined by the polarization direction $\mathbf{e}_i$ and the complex polarizability $\alpha_i(v) = R_i(v) + iI_i(v)$. $I_i(v)$ is obtainable from the experiment, that is from the absorption spectra of the compounds that can be considered good models of the subsystems, and $R_i(v)$ can be calculated from $I_i(v)$ by means of a Kronig–Kramers transform, $v$ is expressed in $cm^{-1}$. More often in order to simplify the calculation, a Lorentzian shape is assumed for an absorption band, so $I_i(v)$ and $R_i(v)$ can be obtained by simple analytical formulae, which require[26] the dipole strength, $\lambda_{max}$ and the band-width. From the general formulation of the DeVoe model, retaining only the terms to first order in $G_{12}$ (physically, this means considering that the electric dipole on the $i$ chromophore is caused by the external e.m. field plus the dipolar fields of the other dipole polarized by the external field only) the following expression can be deduced in the case of two different chromophores having only one electrically allowed transition each, which provides CD as a frequency function is: $\Delta\varepsilon\ (v) = 0.014\ \pi^2 N\mathbf{e}_1 X\mathbf{e}_2 \boldsymbol{R}_{12} G_{12} v^2 [I_1(v)R_2(v) + I_2(v)R_1(v)]$; $G_{12} = (1/r_{12})^3[\mathbf{e}_1.\mathbf{e}_2 - 3(\mathbf{e}_1\mathbf{e}_{12})(\mathbf{e}_2\mathbf{e}_{12})]$. Here $\mathbf{e}_1$, $\mathbf{e}_2$ are the unit direction vectors of the transition dipole moments of the first and second chromophore, respectively, $\boldsymbol{R}_{12}$ is the distance between them and $r_{12}$ its modulus, $G_{12}$ is the point–dipole–point–dipole interaction term and $v$ is the frequency expressed in $cm^{-1}$. This expression gives rise to a couplet-like feature if the absorption maxima of the chromophore 1 and 2 are near in frequency ('quasidegenerate' coupled oscillator system). Of course, for several (say, $n$) oscillators, we shall have, still to the same level of approximation, that is to first order, a sum over $n$ of pairwise interactions, as that reported above. Therefore, in order to obtain, by the DeVoe calculations, $\Delta\varepsilon$ as a frequency function, that is a true theoretical CD spectrum to be compared with the experimental one some input data are required: (i) geometrical parameters, that is the cartesian coordinates of the atoms, which constitute the molecule (if several conformers exist each of them has to be considered), (ii) spectroscopic parameters, that is the absorption characteristics of each of the chromophores, which constitute (+)-**1**. The geometrical input data have been obtained by assuming (a*S*)-absolute configuration for (+)-**1** and carrying out a conformational analysis using the methods of molecular mechanics, that is SPARTAN02 package, MMFF94s force field.[27] In this way, three low-energy conformers have been individuated with energies 64.87, 68.37 and 71.34 kcal/mol. Since the energy differences are 3.50 and 6.47 kcal/mol, only the lowest energy conformer will be appreciably populated and only this one will be considered for our DeVoe calculations. This structure is reported in Figure 4.

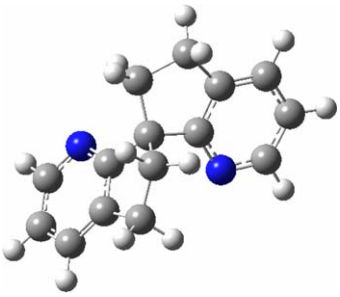

**Figure 4.** The most stable conformer of (a*S*)-**1**, according to MMFF94s calculations.

From a spectroscopic point of view, each pyridine chromophore of **1** has been described by two dipoles in order to represent the transition dipole moments of the $^1A_1 \rightarrow {}^1B_1$ and $^1A_1 \rightarrow {}^1B_2$ transitions, respectively. Thus the former transition has been described by a single oscillator, polarized perpendicularly to the pyridine ring (along the $x$ direction of Chart 1), centred at 270 nm to which a dipolar strength of $3D^2$ has been assigned. The latter transition has been described employing only an oscillator, in the plane of the pyridine ring ($y$ direction of Chart 1) to which a dipolar strength of $6D^2$ has been attributed. The positions (wavelength of the absorption maximum) have been chosen by taking into account that these transitions are substantially degenerate. Hence we decided to locate them in correspondence of the experimental absorption maximum. The values of dipolar strength have been chosen taking into account the experimental UV spectrum of some pyridine derivative[11–13] and to have a correct simulation of the experimental spectrum of **1**. In a first calculation only the dipoles of the $^1A_1 \rightarrow {}^1B_2$ transition were taken into account: in this way a positive couplet (amplitude +15) is obtained. Conversely, the coupling of the dipoles of the $^1A_1 \rightarrow {}^1B_1$ transition gives rise to a negative couplet having a smaller (−3) amplitude. The latter couplet is weaker than the former, however this is not surprising, taking into account that the dipolar strength allied to $^1A_1 \rightarrow {}^1B_1$ transition is smaller than that allied to the $^1A_1 \rightarrow {}^1B_2$ one and, as it is well known,[28] for a dimer of two equal chromophores, at a certain wavelength, the calculated $\Delta\varepsilon$ value is proportional to the square of the $\varepsilon$ value at the same wavelength, which characterizes the chromophore and is used as the input parameter, that is

$$\Delta\varepsilon(\lambda) = \text{const.}\varepsilon^2(\lambda)$$

Finally, when a calculation where all the dipoles (four) were taken into account simultaneously is carried out, the theoretical UV/CD spectra reported in Figure 5 (thick curves) are obtained. In the same figure, the experimental

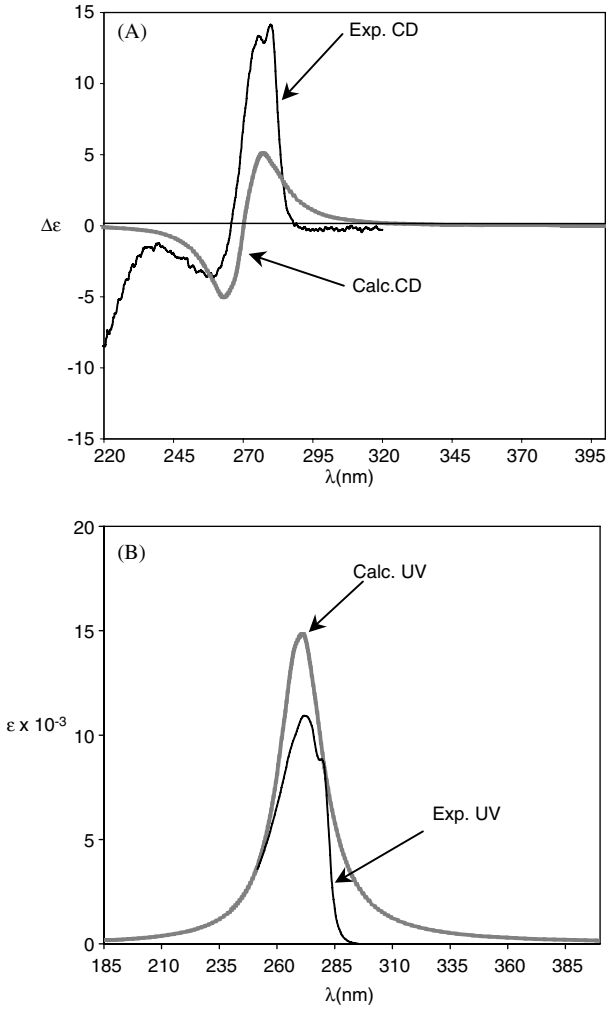


**Figure 5.** (A) Comparison of the experimental (thick curve) and DeVoe calculated (thin curve) CD spectra; (B) Comparison of the experimental (thick curve) and DeVoe calculated (thin curve) UV spectra.

UV/CD spectra (thin curves) are also reported in order to have an easy comparison.

The theoretical CD spectrum reproduces, more than satisfactorily, the sequence of positive/negative Cotton effects observed between 300 and 240 nm: this clearly indicates that the (a*S*)-absolute configuration employed in the calculation is the true configuration of (+)-**1**, that is for this molecule the relationship (+)/(a*S*) still holds. It could be argued that this result was obtained by a coupled oscillator treatment, that is with a method, which takes into account only the electrically allowed transitions and completely neglects the magnetically allowed ones: this fact could constitute an important weak point here, that is in the case of the pyridine chromophore where in the spectral range studied two magnetic dipole allowed transitions are observed.

### 2.5. Density functional theory treatment

In order to overcome this difficulty we decided to tackle this problem by carrying out a more rigorous treatment, that is using the recent density functional theory (DFT) methods,[29–39] as implemented in Gaussian03,[40] for the analysis of the chiroptical properties. First of all we had to find the equilibrium geometry of (a*S*)-**1** to be employed in the CD calculations. For this reason, the geometries of the three structures found previously with the MM calculations have been fully optimized at DFT/B3LYP/6-31G* level. In this way the three structures (represented in Fig. 6) and their energies and relative populations (reported in Table 2) have been found.

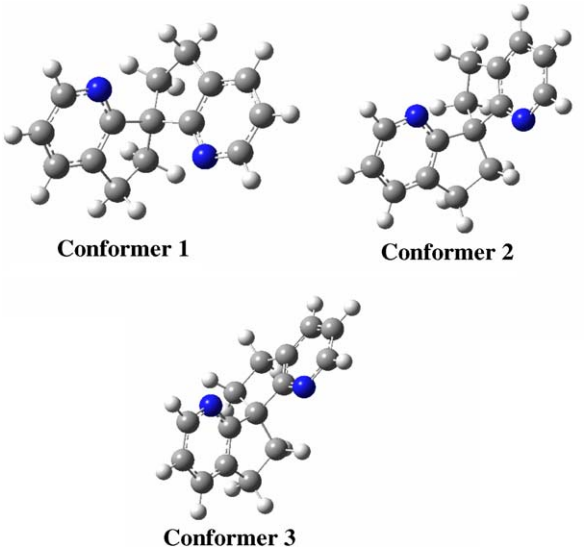


**Figure 6.** The most stable conformers of (a*S*)-**1**, according to DFT/B3LYP/6-31G* calculations.

**Table 2**

| Conformers | Free energy (Hartree) | Free energy difference (kcal/mol) | Boltzmann population (%) |
|---|---|---|---|
| Conformer 1 | −689.322598 | 0 | 78 |
| Conformer 2 | −689.321251 | 0.845255297 | 19 |
| Conformer 3 | −689.319705 | 1.815384983 | 3 |

It is interesting to note how the ab initio geometry optimization changes the energy differences among the conformers: now we have a significant population of a second conformer while that of the third one is small. The CD spectrum of each conformer was calculated (TD DFT/B3LYP/6-31G*) considering the 30 lowest-energy transitions and simulating the experimental spectrum using, for each transition, a Gaussian distribution of the rotatory strength with an half-width value of 0.2 eV.[29]

The theoretical spectrum (Fig. 7, thin line) was finally obtained as a weighted average (taking into account the Boltzmann populations) upon the three conformers and then compared with the experimental CD curve (Fig. 7, thick line). The agreement between the theoretical curve [obtained assuming (a*S*)-absolute configuration] and the experimental one (obtained for **1** in ethanol) indicates the (+)/(a*S*) correlation, strongly supporting our previous result obtained by coupled oscillator calculations.

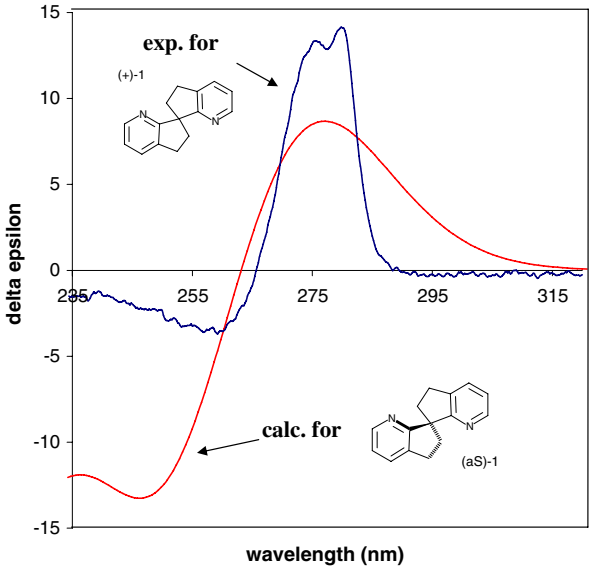


**Figure 7.** Experimental (exp.) CD spectrum of (+)-**1** and TD DFT/B3LYP/6-31G* calculated (calc.) CD spectrum of (a*S*)-**1**.

## 3. Conclusion

The experimental CD spectrum of (+)-**1**, obtained by a semipreparative HPLC resolution upon the CSP Chiralcel AD, shows a positive band (with maxima at 280 and 275 nm) followed by a negative Cotton effect at 260 nm. The shape (number, sign and intensity of the bands) of the spectrum has been reproduced more than satisfactorily, both by using the coupled oscillator model of DeVoe and ab initio methods, assuming (a*S*)-absolute configuration. This establishes the following configurational correlation for **1**: (+)/(a*S*). Taking into account that this correlation has been obtained by two different and completely independent methods, it can be considered as safe.

## 4. Experimental

### 4.1. Instrumental methods and enantioselective columns

The HPLC system consisted of a pump PU 980, with a Rheodyne injector valve equipped with 20 or 100 μL sample loops, a low pressure mixer LG-1580-02 and a line degasser 1550-54 (all from Jasco), a Varian DU-50 spectrophotometer operating at 280 nm and a Varian integrator or Houston Omniscribe recorder for fraction collecting. The polysaccharide derived columns (250 mm × 4.6 mm) were Chiralpak AD (amylose tris-3,5-dimethylphenylcarbamate) and Chiralcel OD (cellulose tris-3,5-dimethylphenylcarbamate) both coated on 10 μm silica gel from Daicel (Tokyo). A column inlet filter with a 0.5 μm stainless steel frit of 3 mm diameter from Rheodyne was used to protect the HPLC columns. Disposable PTFE filters of 0.2 μm pore size were used for filtration of sample solutions. Column void volume ($t_0$) was measured by injection of tri-*tert*-butylbenzene as a non-retained marker.[41] The resolution factor was evaluated according to $R_s = 2(t_2 - t_1)/(w_1 + w_2)$, that is the peak separation divided by the mean value of the baseline widths. Retention times ($t$) were mean values of two replicate determinations. Other HPLC chromatographic parameters were those typically employed.[42] Experiments were performed at ambient temperature. CD spectra were recorded on a Jasco 810 spectropolarimeter using a 1-mm cell. Optical rotations were measured on a Jasco DIP-370 digital polarimeter using a 10-cm microcell.

### 4.2. Computational methods

The geometry optimization has been carried out at the DFT/B3LYP/6-31G* level by means of the Gaussian03 software.[40] All the UV/CD computations have been carried out by means of the Gaussian03 software,[40] employing the TD-DFT approach, the B3LYP functional and the 6-31G* basis set. The rotational strength calculations have been carried out both in velocity and length formalism; the results in the two formalisms are almost identical. The calculated CD spectra in Δε units have been obtained by using overlapping Gaussian functions according to:[29]

$$\Delta\varepsilon(E) = \frac{1}{2.297 \times 10^{-39}} \frac{1}{\sqrt{2\pi}\sigma} \sum_a \Delta E_{0a} R_{0a} e^{-[(E-\Delta E_{0a})/2\sigma]^2}$$

where $\sigma$ is the width of the band at $1/e$ height and $\Delta E_{0a}$ and $R_{0a}$ are the excitation energies and rotational strengths for the transition from 0 to $a$, respectively. The $\sigma$ value is an empirical parameter, and we used the value of 0.15 eV because this gives a good fitting with the experimental width of the bands. The DeVoe calculations were performed by means of a program written by Hug et al.[43] This program is available, free of charge, from the authors of the present article.

## Acknowledgements

Financial support from Università di Catania, Università della Basilicata and MIUR-COFIN2004 (to C.R.) is gratefully acknowledged.

## References

1. Varela, J. A.; Castedo, L.; Saá, C. *Org. Lett.* **1999**, *1*, 2141–2143.
2. Cram, D. J.; Steinberg, H. *J. Am. Chem. Soc.* **1954**, *76*, 2753–2757; Gerlach, H. *Helv. Chim. Acta* **1968**, *51*, 1587.
3. Consiglio, G. A.; Finocchiaro, P.; Failla, S.; Hardcastle, K. I.; Ross, C.; Caccamese, S.; Giudice, G. *Eur. J. Org. Chem.* **1999**, 2799–2806.
4. Caccamese, S.; Principato, G.; Geraci, C.; Neri, P. *Tetrahedron: Asymmetry* **1997**, *8*, 1169–1173.
5. Okamoto, Y.; Yashima, E. *Angew. Chem., Int. Ed. Engl.* **1998**, *37*, 1020–1043.
6. IUPAC Nomenclature of Organic Chemistry, 4th ed.; Pergamon Press: Oxford, 1979; p 489.
7. Eliel, E. L.; Wilen, S. H. *Stereochemistry of Organic Compounds*; Wiley: New York, 1994; p 1121.
8. Kalsi, P. S. *Stereochemistry, Conformation and Mechanism*; Wiley Eastern: New Delhi, 1990; p 86.
9. Cahn, R. S.; Ingold, C.; Prelog, V. *Angew. Chem., Int. Ed. Engl.* **1966**, *5*, 385–415.
10. Overberger, C. G.; Wang, D. W.; Hill, R. K.; Krow, G. R.; Ladner, D. W. *J. Org. Chem.* **1981**, *46*, 2757–2764.

11. Prelog, V.; Helmchem, G. *Angew. Chem., Int. Ed. Engl.* **1982**, *21*, 567–583.
12. Gottarelli, G.; Samori, B. *Tetrahedron Lett.* **1970**, *24*, 2055–2058.
13. Gottarelli, G.; Samori, B. *J. Chem. Soc., Perkin Trans. 12* **1974**, 1462–1465.
14. Smith, H. E.; Schaad, L. J.; Banks, R. B.; Wiant, C. J.; Jordan, C. F. *J. Am. Chem. Soc.* **1973**, *95*, 811–818.
15. Mason, S. F. *Quart. Rev.* **1963**, *17*, 20–66.
16. Mason, S. F. Theory. In *Optical Rotatory Dispersion and Circular Dichroism in Organic Chemistry*; Snatzke, G., Ed.; Wiley and Sons: London, 1967; Chapter 4, p 71.
17. Gottarelli, G.; Mason, S. F.; Torre, G. *J. Chem. Soc. (B)* **1971**, 1349–1353.
18. Hansen, Aa. *Monatsh. Chem.* **2005**, *136*, 253–275; Hansen, Aa. *Monatsh. Chem.* **2005**, *136*, 275–287.
19. Harada, N.; Nakanishi, K. *Acc. Chem. Res.* **1972**, *5*, 257–263.
20. Harada, N.; Nakanishi, K. *Circular Dichroic Spectroscopy: Exciton Coupling in Organic Stereochemistry*; University Science Books: Mill Valley, CA, 1983.
21. Nakanishi, K.; Berova, N. In *Circular Dichroism: Principles and Applications*; Nakanishi, K., Berova, N., Woody, R. W., Eds.; VCH Publishers: New York, 1994; Chapter 13, p 361.
22. Nakanishi, K.; Berova, N. In *Circular Dichroism: Principles and Applications*; Nakanishi, K., Berova, N., Woody, R. W., Eds.; Wiley-VCH Publishers: New York, 2000; Chapter 12, p 337.
23. DeVoe, H. *J. Chem. Phys.* **1965**, *43*, 3199–3208.
24. Rosini, C.; Salvadori, P.; Zandomeneghi, M. *Tetrahedron: Asymmetry* **1993**, *4*, 545–554.
25. Superchi, S.; Giorgio, E.; Rosini, C. *Chirality* **2004**, *16*, 422–451.
26. Cech, C. L.; Hug, W.; Tinoco, I., Jr. *Biopolymers* **1976**, *15*, 131–152.
27. SPARTAN '02, Wavefunction Inc. 18401 Von Karman Avenue, Suite 370, Irvine, CA 92612, 2002, http://www.wavefun.com/.
28. Zandomeneghi, M.; Rosini, C.; Salvadori, P. *Chem. Phys. Lett.* **1976**, *44*, 533–536.
29. Diedrich, C.; Grimme, S. *J. Phys. Chem. A* **2003**, *107*, 2524–2539.
30. Autschbach, J.; Ziegler, T.; van Gisbergen, S. J. A.; Baerends, E. J. *J. Chem. Phys.* **2002**, *116*, 6930–6940.
31. Pecul, M.; Ruud, K.; Helgaker, T. *Chem. Phys. Lett.* **2004**, *388*, 110–119.
32. Grimme, S.; Bahlmann, A. *Modern Cyclophane Chem.* **2004**, 311–336.
33. Braun, M.; Hohmann, A.; Rahematpura, J.; Buehne, C.; Grimme, S. *Chem. Eur. J.* **2004**, *10*, 4584–4593.
34. Furche, F.; Ahlrichs, R.; Wachsmann, C.; Weber, E.; Sobanski, A.; Voegtle, F.; Grimme, S. *J. Am. Chem. Soc.* **2000**, *122*, 1717–1724.
35. Stephens, P. J.; McCann, D. M.; Butkus, E.; Stoncius, S.; Cheeseman, J. R.; Frisch, M. J. *J. Org. Chem.* **2004**, *69*, 1948–1958.
36. Stephens, P. J.; McCann, D. M.; Devlin, F. J.; Cheeseman, J. R.; Frisch, M. J. *J. Am. Chem. Soc.* **2004**, *126*, 7514–7521.
37. Neugebauer, J.; Baerends, E. J.; Nooijen, M.; Autschbach, J. *J. Chem. Phys.* **2005**, *122*, 234305/1–234305/7.
38. Pecul, M.; Marchesan, D.; Ruud, K.; Coriani, S. *J. Chem. Phys.* **2005**, *122*, 024106/1–024106/9.
39. Giorgio, E.; Tanaka, K.; Ding, W.; Krishnamurthy, G.; Pitts, K.; Ellestad, G. A.; Rosini, C.; Berova, N. *Bioorg. Med. Chem.* **2005**, *13*, 5072–5079.
40. Frisch, M. J.; Trucks, G. W.; Schlegel, H. B.; Scuseria, G. E.; Robb, M. A.; Cheeseman, J. R.; Zakrzewski, V. G.; Montgomery, J. A., Jr.; Stratmann, R. E.; Burant, J. C.; Dapprich, S.; Millam, J. M.; Daniels, A. D.; Kudin, K. N.; Strain, M. C.; Farkas, O.; Tomasi, J.; Barone, V.; Cossi, M.; Cammi, R.; Mennucci, B.; Pomelli, C.; Adamo, C.; Clifford, S.; Ochterski, J.; Petersson, G. A.; Ayala, P. Y.; Cui, Q.; Morokuma, K.; Malick, D. K.; Rabuck, A. D.; Raghavachari, K.; Foresman, J. B.; Cioslowski, J.; Ortiz, J. V.; Stefanov, B. B.; Liu, G.; Liashenko, A.; Piskorz, P.; Komaromi, I.; Gomperts, R.; Martin, R. L.; Fox, D. J.; Keith, T.; Al-Laham, M. A.; Peng, C. Y.; Nanayakkara, A.; Gonzalez, C.; Challacombe, M.; Gill, P. M. W.; Johnson, B. G.; Chen, W.; Wong, M. W.; Andres, J. L.; Head-Gordon, M.; Replogle, E. S.; Pople, J. A. *Gaussian*. Gaussian: Pittsburgh, PA, USA.
41. Koller, H.; Rimböck, K.-E. *J. Chromatogr.* **1983**, *282*, 89–94.
42. Allenmark, S. *Chromatographic Enantioseparation: Methods and Applications*, 2nd ed.; Ellis Horwood: Chichester, 1991; p 82.
43. Hug, W.; Ciardelli, F.; Tinoco, I. *J. Am. Chem. Soc.* **1974**, *96*, 3407–3410.